

Dynamo Line Simulation using a Hot Dip Process Simulator

**E. J. Hilinski (1), G. N. Walters (1), R. H. Wolf (1),
J. Huňady (2), A. Magurova (2), and M. Predmerský (2)**

*(1) U. S. Steel Research and Technology Center, 4000 Tech Center Drive, Monroeville,
Pennsylvania, 15146, USA*

*(2) U. S. Steel Košice, Research and Development Center, Vstupny areal U. S. Steel, 44 55,
Košice, Slovakia*

Abstract

Newly developed processing routines on U. S. Steel's Hot Dip Process Simulator (HDPS) have enabled accurate simulation of the operating characteristics of a continuous electrical sheet processing line. The two key components of the electrical steel production process simulated were decarburization and grain growth. As the HDPS cannot process panels of a size adequate for obtaining longitudinal and transverse mini-frame (16.5 cm long) Epstein packs, new coupon test techniques for magnetic property measurement were required. Magnetic properties measured on coupons tested in a small single sheet tester were correlated to those measured on full size (30.5 cm long) Epstein packs. Reasonable agreement between the Epstein and coupon properties was achieved. Magnetic properties obtained via laboratory processing and testing have agreed with those from mill processing and testing. The HDPS electrical steel simulations are now being used to more fully explore the processing-microstructure-property interrelationships in continuously annealed electrical steels

Introduction.

U. S. Steel's graduation from a regional to a global steel producing company via the purchase of the former VSZ steel plant in the Slovak Republic reintroduced fully processed electrical steels (FPES) into its cadre of products. VSZ, now named U. S. Steel—Košice (USSK), had been producing about 150,000 metric tons of FPES per year in grades ranging from M800 to M470 in sheet thicknesses of 0.50 and 0.65 mm on two Dynamo Lines. Lower core loss grades could not be reliably produced because of equipment and design limitations in these two lines. For that reason, and because of a burgeoning market for electrical steels in Central and Eastern Europe, USSK recently commissioned a new Dynamo Line expected to produce another 100,000 metric tons per year of electrical steel. Some of the grades to be produced on the new line will be low core loss grades, M300, M350, and M400 in sheet thickness of 0.50 mm and in some cases in thicknesses of 0.35 mm.

A key initiative, therefore, is development of low core loss grades for the new Dynamo Line as well as high permeability grades. The first two of these products that were produced in 2004 were the high permeability grades M800-65AP and M700-50AP. In addition, production trials of the M400-50A grade have been successfully run on the new Dynamo Line while it was being commissioned. A critical component of the development activities was development of Dynamo Line simulation capabilities on U. S. Steel's hot dip process simulator (HDPS). The development of the processing and test techniques required to accurately simulate Dynamo Line production is the subject of this paper.

Description of the HDPS.

The U. S. Steel HDPS was designed to meet or exceed the capabilities of any of the U. S. Steel continuous galvanizing lines (CGLs) currently in operation, with the exception of production rate. It can produce a steel sample with a thermal history matching any CGL design at any line speed with a variety of coatings. A command

based program structure allows modifications of any part of the cycle, including changes to the atmosphere and dew point while annealing. Furthermore, it allows for experiments that cannot be conducted at commercial facilities such as interrupting and retrieving a sample from any part of the process cycle or testing the effects of a new piece of equipment prior to actually installing it on a production line. While not originally designed to simulate USSK's Dynamo Lines, the extensive capabilities of the HDPS made this possible with essentially no modification to either hardware or software.

A schematic and photograph of the main sections of the HDPS are provided in Figure 1. The HDPS is a vertical system, which transfers the steel sample (attached to a drive rod) up and down through various processing sections. The support structure for the drive rod is mounted at the top of the main column of the simulator. It is manipulated up and down by a screw mechanism with fine position control. The steel sample is hung on the drive rod through the sample

entry/cooling chamber. Below this chamber is an IR furnace with 9 quartz lamps on each side separated vertically into 3 heating zones. The lamps heat the steel sample through a 16 cm diameter transparent quartz tube that is approximately 60 cm tall. At the base of the upper chamber is an induction furnace, which is comprised of two water-cooled copper coils. The upper chamber is separated from the lower chamber by an atmosphere-sealing gate valve, which is only opened seconds before a sample is transferred into the molten metal bath. This gate valve allows annealing cycles to be run without dipping, thereby eliminating the effort associated with mounting a pot, and also helps to keep the rest of the simulator column relatively free of zinc dust. As none of the electrical steel samples were zinc coated, all of the Dynamo Line simulations were conducted with this gate valve closed.

For material to be zinc coated, a set of rollers located below the gate valve helps guide the steel sample through the wiping knives that hang within centimeters of the surface of the molten

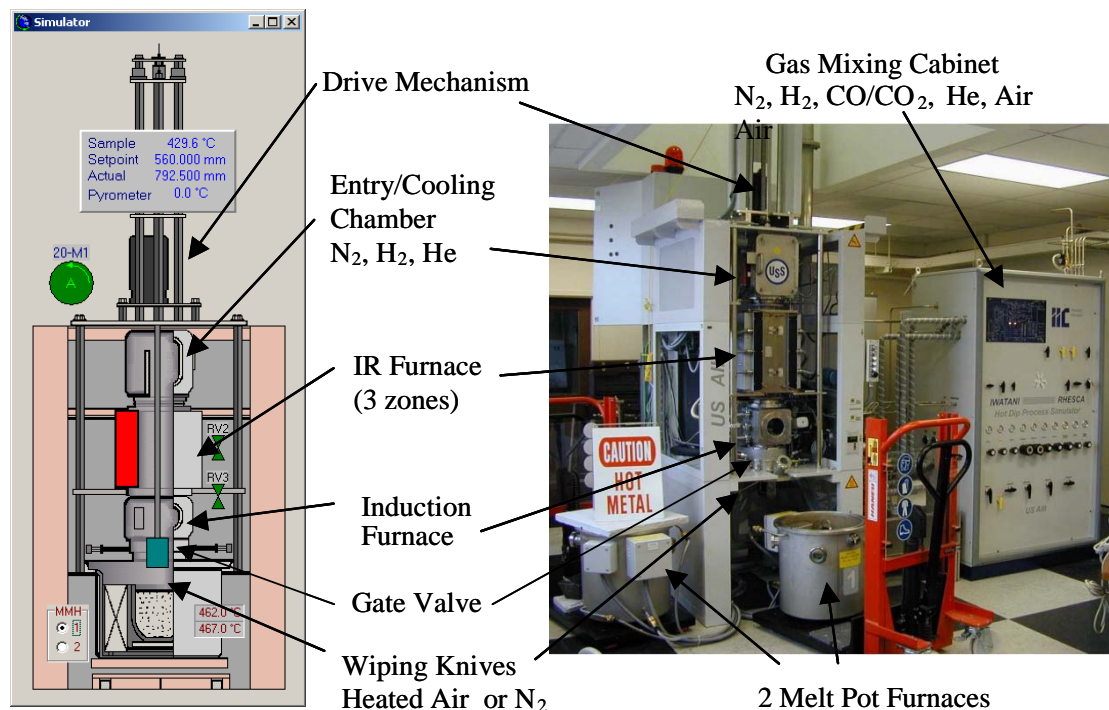


Figure 1. Schematic diagram and photograph of the U. S. Steel Research HDPS.

metal when a pot furnace is mounted. Two different melt pot furnaces can be bolted to the bottom of the simulator. These pots are independently controlled so that one pot can be run on the simulator while the melt in the other pot is prepared. To the right of the simulator stands a gas mixing cabinet which contains 19 automated mass flow controllers and is currently capable of supplying 5 different gas types. The gases may be humidified in a heated water bath which is placed between the main column of the simulator and the gas mixing cabinet. Not visible in Figure 1, but integral to operations, are two computer control cabinets, a cooling system and two induction control cabinets.

Table 1 provides some of the relevant performance capabilities of the HDPS. As noted, the overall HDPS sample size is 120 mm by 215 mm, which yields a uniform area of 80 mm by 90 mm for coating and mechanical properties. Appropriate furnace tuning prior to experimentation keeps the temperature variation in this uniform area to about $\pm 10^{\circ}\text{C}$ from the desired annealing temperature. The total working volume of controlled atmosphere in the simulator is approximately 35 liters. This small volume is advantageous for making rapid changes to the dew point and/or composition of the atmosphere during an annealing cycle. This is a very useful feature because USSK's Dynamo Lines have two furnace sections requiring different atmospheres. First, the incoming strip is heated to about 825 to 850°C where decarburization is accomplished in a wet HNX atmosphere. Then the strip passes through the grain growth anneal which requires dry HNX gas. On the HDPS the decarburization anneal was typically carried out in HNX gas with a dew point of 20°C and the atmosphere rapidly exchanged with dry HNX enabling the grain growth anneal to be conducted in dry HNX with a dew point ranging from -20 to -30°C. Similar to the fifty-foot process record of a CGL, the HDPS monitors over 54 parameters such as the temperatures from 12 thermocouples, gas flows from 19 mass flow controllers, power settings, position sensors, dew points and pressures from 4 pressure gauges. The data collection interval of these parameters can be as low as 20 milliseconds.

Table 1. Capabilities of the USS Research HDPS.

Sample size	120 mm x 215 mm (4.75 in x 8.5 in)
Gauge range	0.25 mm - 3.0 mm (0.01 in - 0.12 in)
Uniformly coated area	> 80 mm x 90 mm (3.15 in x 3.5 in)
IR furnace	1000°C (1832°F) max at 50°C/sec [‡]
Induction furnace	Curie Temp. (767°C) at 100°C/sec [‡]
Cooling rate	70°C/sec (125°F/sec) [‡]
Dew point control	- 50°C → + 25°C (- 58°F → + 77°F)
Wiping knives	Heated N ₂ or Air 15-200 g/m ² /side
Withdraw speed	1300 mm/sec (255 fpm)
Melting pots	800°C max (1472°F max), at 250°C/hr (450°F/hr)
Melt capacity	34 kg (75 lb) Zn, 18 kg (40 lb) 55% Al-Zn

[‡] for a 0.7 mm (0.028 in) gage

Magnetic Testing of Small Coupons.

Unfortunately, the uniform area of the HDPS sample panel does not contain nearly enough material to produce even mini-frame (16.5 cm long) Epstein strips. Therefore, a Soken DAC-BHW5 small single sheet tester was used to evaluate magnetic properties. A correlation was needed between full-size (30.5 cm long) Epstein pack and Soken coupons test samples. Successful development of such a correlation for semi-processed CRML steels by⁽¹⁾ indicated that a meaningful correlation was possible. USSK provided full width, 1000 mm (40 in.), by about 500 mm (20 in.) long sheet samples from all of their current production grades. These sheet samples represent eight different grade and gage combinations, as outlined in Table 2. The approach was to correlate the test data from one Epstein pack tested on a Donart model 3110-MS2 Epstein tester to a standardized 76.2 by 76.2 mm (3 by 3 in.) Soken coupon of companion material sheared from the same sheet. These dimensions were used so that almost all of 80 by 90 mm

Table 2. Listing of the USSK Sheet Samples Provided for Correlation.

Product	Nom. Gage [mm]	Act. Gage [mm]	Test Density [g/cm ³]
M800-65A	0.65	0.661	7.80
M800-50A	0.50	0.496	7.80
M700-65A	0.65	0.629	7.80
M700-50A	0.50	0.488	7.80
M600-65A	0.65	0.662	7.75
M530-65A	0.65	0.647	7.70
M530-50A	0.50	0.498	7.70
M470-50A	0.50	0.507	7.70

uniform heating area of the HDPS sample was covered. Standardization of sample size is important as the magnetic properties are expected to vary with sample size in fully processed electrical steels. These steels are tested with edge strain left from shearing or punching in the test piece. As the sample becomes smaller, especially in the width direction, the fraction of strained to unstrained material increases, causing the magnetic properties to vary. Perhaps a better correlation method would have been to test an Epstein pack of the subject material on the Donart Epstein tester and then test each strip of the same pack on the Soken Tester. This type of correlation will be undertaken in future work.

Correlation Testing Procedures.

One full size (30.5 cm) Epstein pack composed of 12 longitudinal (L) and 12 transverse (T) strips was sheared along with one 76.2 by 76.2 mm coupon from each sheet of USSK production material. The Epstein packs were tested on a Donart 3110-MS2 core loss console using an exciting current frequency of 50 Hz. Both the L and T half packs along with the full L and T composite packs were tested. Full 40 point B-H curve data were obtained over a magnetic flux density range of 0.05 – 1.90 Tesla. In addition, the magnetic flux density values were recorded at magnetic field strength values of 800, 2500, 5000, and 10000 A/m, namely the B_{800} , B_{2500} , B_{5000} , and B_{10000} values that are used to determine the magnetic polarizations J_{800} , J_{2500} , J_{5000} , and J_{10000} .

The sample test density was calculated according to the relationship given in ASTM specification A34, “Standard Practice for Sampling and Procurement Testing of Magnetic Materials.” The values of test density used for each grade are listed in Table 2.

The corresponding coupons were then tested on the Soken tester. First the coupon was weighed to the nearest 0.01 gram. Then the longitudinal and transverse direction widths were measured to the nearest 0.001 in. and converted to millimeters. The theoretical sample gage was then calculated by using the width dimensions, the weight, and the test density. The theoretical sample gage and the appropriate width (for the L or T direction) were input into the Soken tester. The core losses and magnetic field strengths were recorded at the same magnetic flux density levels as used in the 40 point B-H curve Epstein testing. The Soken tester was then switched into H-control mode to allow testing for the B_{800} , B_{2500} , and B_{5000} values. Because the Soken tester’s power supply was not able to generate magnetic flux densities above 1.7 Tesla, B_{10000} values were not obtained. All Soken testing was also conducted with an exciting current frequency of 50 Hz.

Correlation Testing Results.

The longitudinal and transverse core loss results for all grades were compared and are shown in Figure 2. The correlation between the Soken and Epstein tests are linear and nearly the same for longitudinal and transverse directions. Because the longitudinal and transverse core losses are measured separately, it was decided to use separate correlations for each. The core loss correlation results were separated by gage and are shown in Figure 3 for the longitudinal core loss correlation. A similar behavior was observed for the transverse core loss. Obviously, gage has an effect on the core loss correlation that cannot be ignored. Finally, for each distinct gage, the effect of alloy content on the core loss was examined. Figure 4 shows this result for the longitudinal core loss in 0.50 mm thick material. In this case as well as the others, longitudinal and transverse core losses in 0.50 and 0.65 mm material, the effect of grade was

slight and non-linear. There was no clear monotonically increasing or decreasing trend to the data as a function of grade. Therefore, a common

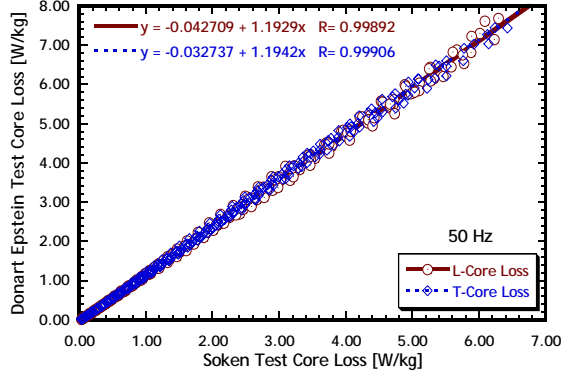


Figure 2. Correlation of the Soken to Epstein test longitudinal at transverse core losses measured at 50 Hz for all grades and gages and with a linear curve.

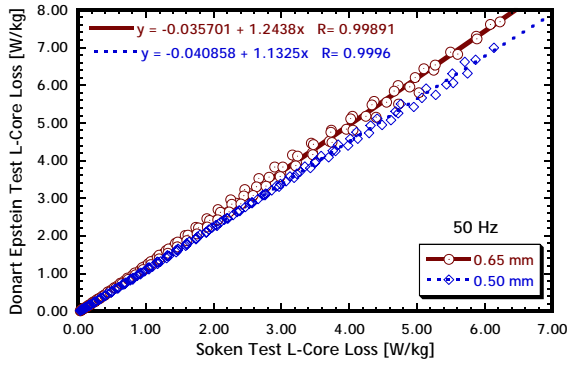


Figure 3. Correlation of the Soken to Epstein test longitudinal core losses measured at 50 Hz separated by gage for all grades.

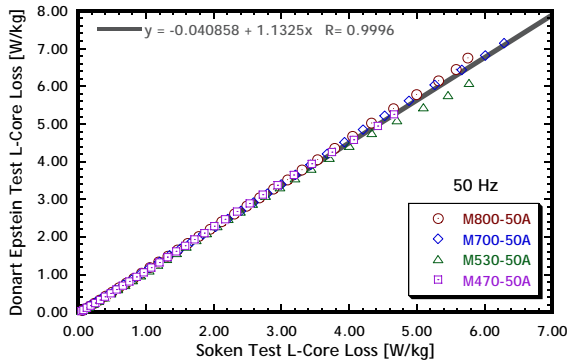


Figure 4. Correlation of the Soken to Epstein test longitudinal core losses measured at 50 Hz separated by grade for the 0.50 mm thick material.

linear correlation is used to fit the core loss data independent of grade. Only the material gage and test orientation (longitudinal and transverse) is considered. The resulting correlation equations are shown in Table 3 for core loss and magnetic flux density.

Table 3. Summary of the Correlation Equations for USSK Fully Processed Material.

Property	Orientation	Relation
0.65 mm sample thickness		
Core Loss	Longitudinal	$P_{EpL} = -0.035701 + 1.2438 \cdot P_{S_L}$
Core Loss	Transverse	$P_{EpT} = -0.024251 + 1.2077 \cdot P_{S_T}$
Magnetic Flux Density	Longitudinal	$B_{EpL} = -0.26351 + 1.1464 \cdot B_{S_L}$
Magnetic Flux Density	Transverse	$B_{EpT} = -0.21088 + 1.1286 \cdot B_{S_T}$
0.50 mm sample thickness		
Core Loss	Longitudinal	$P_{EpL} = -0.040858 + 1.1325 \cdot P_{S_L}$
Core Loss	Transverse	$P_{EpT} = -0.025868 + 1.1603 \cdot P_{S_T}$
Magnetic Flux Density	Longitudinal	$B_{EpL} = -0.11449 + 1.0662 \cdot B_{S_L}$
Magnetic Flux Density	Transverse	$B_{EpT} = -0.12956 + 1.0757 \cdot B_{S_T}$

Nomenclature: P_{EpL} : Longitudinal Epstein Core Loss
 P_{EpT} : Transverse Epstein Core Loss
 B_{EpL} : Longitudinal Epstein Magnetic Flux Density
 B_{EpT} : Transverse Epstein Magnetic Flux Density
 P_{S_L} : Longitudinal Soken Core Loss
 P_{S_T} : Transverse Soken Core Loss
 B_{S_L} : Longitudinal Soken Magnetic Flux Density
 B_{S_T} : Transverse Soken Magnetic Flux Density

A similar approach was used in analyzing the magnetic flux density data, B_{800} , B_{2500} , and B_{5000} . First, all of the data was graphed together as shown in Figure 5. It is evident that the longitudinal and transverse data can be described by almost the same linear curve. This was found to be the case for sample gage as well, as is shown in Figure 6 for the longitudinal magnetic flux density. An analysis of the data as a function of gage and test orientation with grade separated was conducted and an example is shown in Figure 7 for the transverse magnetic flux density in 0.50 mm thick material. In every case the data clusters are about a

common line except for the M800 grade. As this correlation was being developed for analysis of more highly alloyed experimental M400-50A samples, it was decided to eliminate the M800 grade data from the correlation and use only the data from the more highly alloyed grades. The resulting linear correlations, therefore, do not use the M800 data. Table 3 also summarizes the resulting correlation equations for longitudinal and transverse magnetic flux density at each gage.

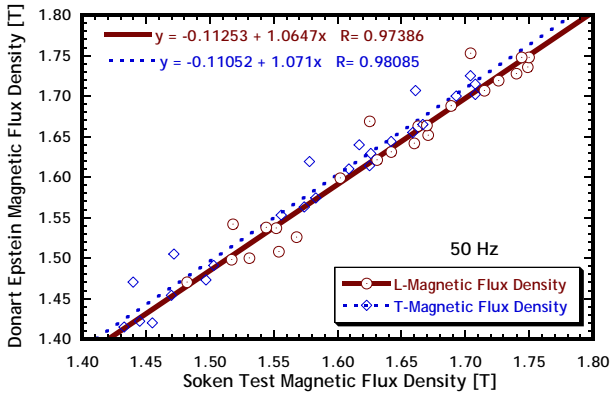


Figure 5. Correlation of the Soken to Epstein test longitudinal and transverse magnetic flux densities measured at 50 Hz for all grades and gages and fit with a linear curve.

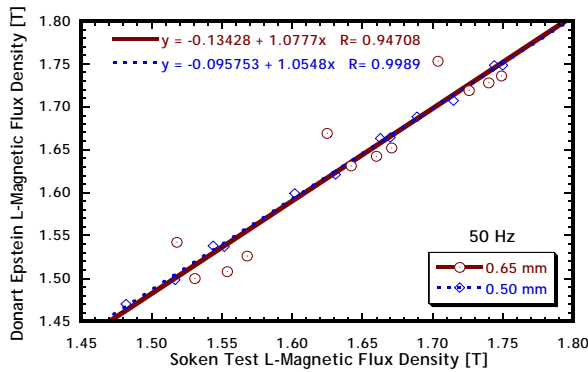


Figure 6. Correlation of the Soken to Epstein test longitudinal magnetic flux density measured at 50 Hz separated by gage for all grades.

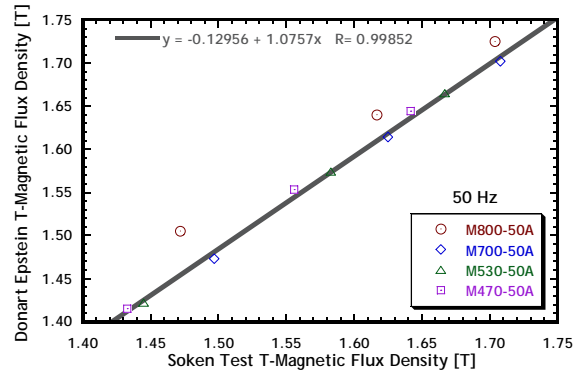


Figure 7. Correlation of the Soken to Epstein test transverse magnetic flux density measured at 50 Hz separated by grade for the 0.50 mm thick material.

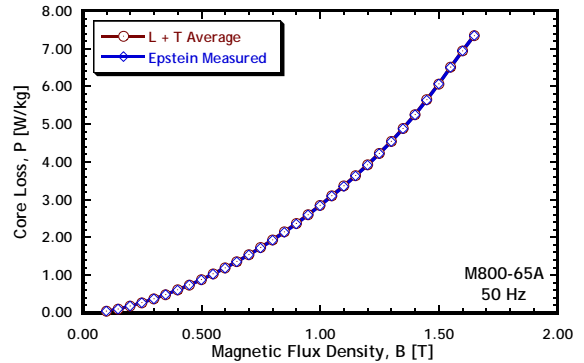


Figure 8a. Comparison of the measured Epstein L + T composite pack core loss to the average of the L and T Epstein core losses for grade M800-65A.

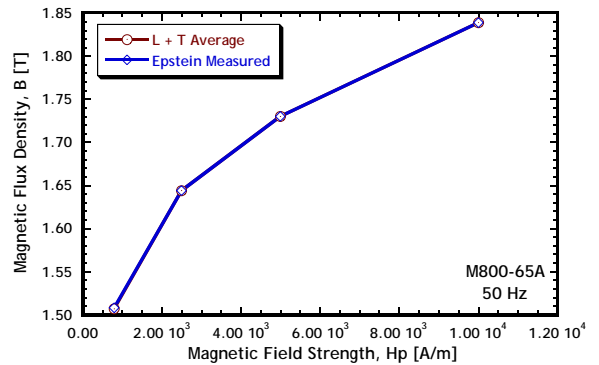


Figure 8b. Comparison of the measured Epstein L + T composite pack flux density to the average of the L and T Epstein flux densities for grade M800-65A.

Once the corrected values for longitudinal and transverse core losses and magnetic flux densities are obtained, they are converted into composite L and T Epstein pack results by arithmetically averaging the L and T properties. The validity of this approach is supported by the results shown in Figures 8a and 8b for the M800-65A grade core loss and magnetic flux density respectively. The average and measured curves are nearly identical. The maximum per-cent difference in measured and arithmetically averaged core loss for all the grades over a magnetic flux density range of 0.05 to 1.9 T was 6.5% with a

corresponding maximum average deviation over all flux density levels of 3.7%. This was for the M470-50A grade. The differences in magnetic flux density are much better than core loss, generally under 1%. Finally, the correlations were applied to the measured Soken coupon data and L and T composite Epstein properties. The 1 and 1.5 T core losses and the B_{800} , B_{2500} , and B_{5000} , magnetic flux densities were predicted. These results were compared to the measured Epstein results and are presented in Table 4. It can be seen that the average deviation (for all grades) in these values for core loss is within 2% and that for magnetic flux density is below 0.5%.

Table 4. Soken Epstein Equivalent Results Compared to the Measured Epstein Results at 50 Hz

Grade	$P_{1.0s}$ [W/kg]	$P_{1.0E}$ [W/kg]	% Diff.	$P_{1.5s}$ [W/kg]	$P_{1.5E}$ [W/kg]	% Diff.	B_{25s} [T]	B_{25E} [T]	% Diff.	B_{50s} [T]	B_{50E} [T]	% Diff.		
M700-65A	2.63	2.68	1.87	5.89	5.98	1.51	1.628	1.640	0.73	1.729	1.725	0.23		
M700-50A	2.70	2.74	1.46	5.69	5.84	2.57	1.639	1.638	0.06	1.726	1.724	0.12		
M600-65A	2.43	2.46	1.22	5.12	5.24	2.29	1.622	1.621	0.06	1.716	1.709	0.41		
M530-65A	2.15	2.15	0.00	4.75	4.69	1.28	1.592	1.597	0.31	1.688	1.687	0.06		
M530-50A	2.37	2.31	2.60	5.05	4.91	2.85	1.599	1.598	0.06	1.689	1.685	0.24		
M470-50A	1.99	2.08	4.33	4.46	4.52	1.33	1.569	1.576	0.44	1.662	1.666	0.24		
Average:			1.91	Average:			1.97	Average:			0.28	Average:		0.22

HDPS Dynamo Line Annealing Cycle Development.

The HDPS simulation of USSK's Dynamo Line 3 was conducted in two phases. The first phase focused on developing a simulation for the grain growth anneal. In the second phase, the decarburization cycle was simulated and added to the grain growth cycle anneal. The implementation of these simulations were used to guide Dynamo Line 3 setups for development of the first low core loss grade to be produced by USSK, M400-50A.

HDPS Dynamo Line Grain Growth Simulation—Experimental Procedures.

Full-width sheet samples from the head, middle, and tail from one coil of the experimental M400-50A grade were collected following decarburization annealing on USSK's Dynamo Line 2. This line has a temper mill between the

decarburization and grain growth furnaces that provides an excellent location for collecting decarburized sheet samples. Table 5 shows the chemical composition of this material. The electromagnetic properties of the decarburized sheet samples were measured at USSK on full-size (28-cm) Epstein packs composed of an equal number of strips oriented parallel (L) and transverse (T) to the rolling direction. Sheet samples were sent to the Monroeville Research and Technology Center and were used as starting material for a study on the grain growth annealing characteristics. The sheet samples were sheared into HDPS sample panels that were

Table 5. Chemical Composition of the Commercial M400-50A Material, in weight percent.

C	Mn	P	S	Si	Al	N ₂	O ₂
0098	0.26	0.016	0.0048	2.38	0.39	0.002	0.0023

203.2 mm (8 in.) long by 127 mm (5 in.) wide. Table 6 shows the time-temperature parameters, based on the operating parameters of Dynamo Line 3, that were used for the simulated grain growth anneal. In practice, the HDPS successfully processed samples up to a strip temperature of 1045°C in a dry (-40°C) 5% H₂ balance N₂ atmosphere to avoid deterioration in the magnetic properties due to subsurface oxidation. After the anneal simulation, Soken coupons of 76.2 by 76.2 mm (3 in. by 3 in.) dimensions were sheared from the center

of the panels for electromagnetic property measurement on the single sheet Soken Tester. The measured Soken values of longitudinal and transverse core loss and polarization were then converted to equivalent Epstein values via the correlations shown in Table 3. Finally, metallographic analysis for grain size was performed to complete the process—property—microstructure interrelationships of the grain growth anneal for this experimental M400-50A grade.

Table 6. Time-Temperature Parameters Used for Grain Growth Anneal on the HDPS.

Process	Heating Time [s]	Soak Temp. [°C]	Soak Time [s]	Corresponding DN #3 Line Speed [m/min]	Cooling Time to 650°C [s]	Cooling Time 650 to 50°C [s]
1	74		29	40	45	44
2	60		23	50	36	36
3	50	900	19	60	30	30
4	43		17	70	26	25
5	37		15	80	23	22
6	74		29	40	45	44
7	60		23	50	36	36
8	50	950	19	60	30	30
9	43		17	70	26	25
10	37		15	80	23	22
11	74		29	40	45	44
12	60		23	50	36	36
13	50	1000	19	60	30	30
14	43		17	70	26	25
15	37		15	80	23	22
16	74		29	40	45	44
17	60		23	50	36	36
18	50	1045	19	60	30	30
19	43		17	70	26	25
20	37		15	80	23	22

Notes—(1) Annealing atmosphere: 5% H₂ balance N₂, dry (-40°C dew point).
(2) Nominal sample thickness: 0.50 mm (0.0197 in.).

HDPS Dynamo Line Grain Growth Simulation—Results and Discussion.

The post-decarburization intermediate $P_{1.5}$ core losses ranged from 4.61 to 4.72 W/kg. This result was expected as the ferrite grain size following the 830°C decarburization anneal was simply too small to give core losses below the required 4.00 W/kg level for this grade, as shown in Figure 9. After the samples were tested, they were aged at 225°C for 24 hours and then the properties were measured again and the aging index was calculated. In all cases the aging index was zero, indicating the decarburization anneal was successful in removing carbon to a non-magnetic aging level.

The grain growth anneal simulation on the HDPS yielded the magnetic properties that are summarized in Figures 10a to 11b. The anneal soak times were determined based upon the grain growth furnace length in Dynamo Line 3 and a range of possible line speeds which are listed in Table 6. The annealing time-temperature-property results shows that increasing the temperature of the grain growth anneal and prolonging the soaking time decreases core losses. The initial value of the $P_{1.5}$ core loss of 4.66 W/kg (the average from the head, middle and tail coil locations after decarburization) were reduced to 3.38 to 4.29 W/kg depending upon the annealing condition as shown in Figure 10b.

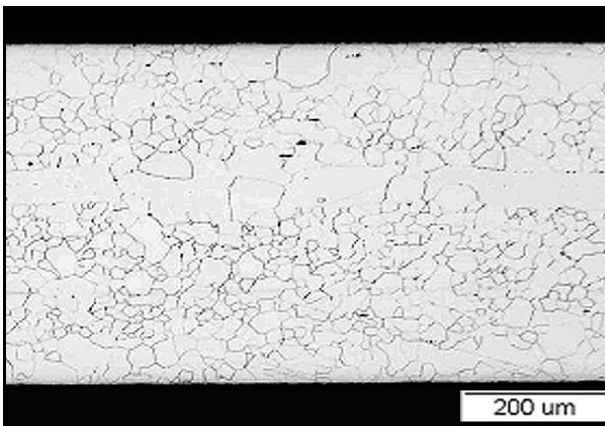


Figure 9. The post-decarburization anneal microstructure.

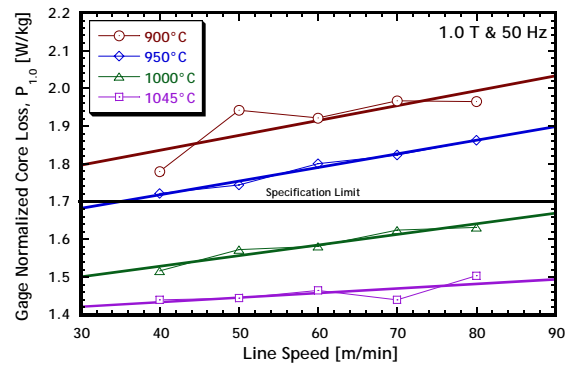


Figure 10a. The effect of line speed (soak time) and soak temperature of the grain growth anneal on the $P_{1.0}$ core loss.

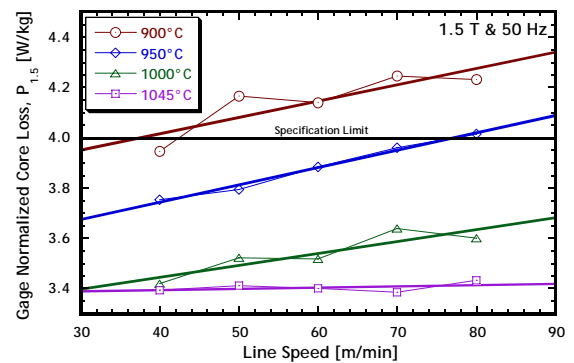


Figure 10b. The effect of line speed (soak time) and soak temperature of the grain growth anneal on the $P_{1.5}$ core loss.

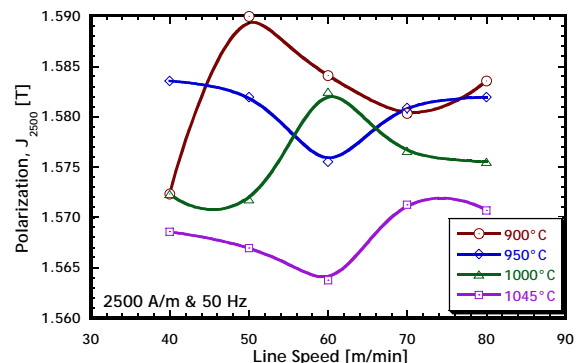


Figure 11a. The effect of line speed (soak time) and soak temperature of the grain growth anneal on the J_{2500} magnetic polarization.

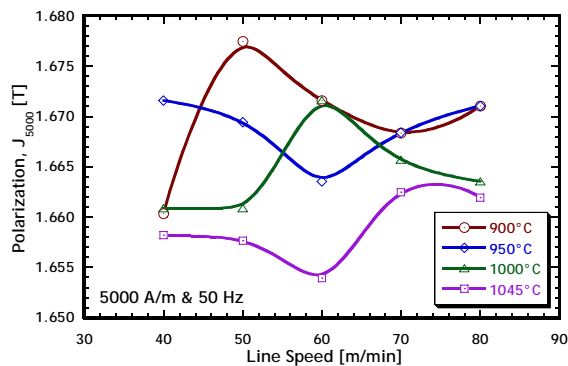


Figure 11b. The effect of line speed (soak time) and soak temperature of the grain growth anneal on the J_{5000} magnetic polarization.

It is expected that a typical core loss of 3.50 to 3.60 W/kg is required to robustly meet the 4.00 W/kg maximum. It is for this reason that the grain growth annealing temperature of 950°C is not sufficient even though for line speeds of 40 to 70 m/min. core losses below 4.00 W/kg were obtained. Based upon this criteria and considering the data presented in Figure 10b, a 1000°C soak temperature is sufficient to produce acceptable core losses for line speeds less than 70 m/min. To run Dynamo Line 3 at its practical maximum speed of 80 m/min, an estimated soak temperature of about 1025°C is required. It is worth noting that the annealing temperature of 900°C does not produce sub-4.00 W/kg core losses at any line speed other than 40 m/min. The effect of soak time on core loss is not especially strong, as increasing the line speed from 40 to 80 m/min only increases core losses by about 0.3 W/kg.

Interestingly, the more difficult core loss specification for this grade is the 1.70 W/kg maximum $P_{1.0}$ core loss. The results for $P_{1.0}$ core loss are shown in Figure 10a. The same trends noted for the $P_{1.5}$ core loss behavior hold here as well. In this case, none of the 950°C test samples meet the specification. The Euronorm specifications for the J_{2500} , J_{5000} , and J_{10000} magnetic polarizations in M400-50A are, respectively, 1.53, 1.63, and 1.73 T at corresponding magnetic field strengths of 2500, 5000, and 10000 A/m.

Unfortunately, the Soken Tester does not have a strong enough power supply to allow testing at magnetic field strengths greater than 5000 A/m therefore the J_{10000} data could not be determined. For J_{2500} and J_{5000} however, all of the grain growth annealing conditions produced magnetic flux density values substantially above the minimum specified levels as shown in Figures 11a and 11b, respectively. Furthermore, the J_{5000} magnetic flux density is almost always the most difficult to meet, so it is expected that the J_{10000} magnetic flux density is met by all of the grain growth annealing conditions.

The resultant microstructures from the center and one corner of the 3 in. by 3 in. Soken test coupon following the grain growth anneal were examined to see if there was a significant grain size difference (indicating a significant temperature difference) across the test coupon. A typical example of this comparison is shown in Figures 12a and 12b. After all of the comparisons were examined, it was concluded that the grain size difference was slight and not significant. Therefore, the magnetic property variability within the coupon due to grain size differences is not believed to be significant. Typical microstructures, taken from the center of the Soken test coupons, at selected times and temperatures can be seen in Figures 12a, 12c, and 12d. It is clear when comparing the microstructures in Figures 12 to those in Figure 9 that additional grain growth occurred in the anneal simulation. The decarburized grain size is estimated to be about 20 μm via optical image analysis, whereas the grain size range in the annealed samples was estimated to range from about 23 μm to 70 μm . In reviewing all of the magnetic property information presented in Figures 10a to 11b, the estimated strip temperature for the Dynamo Line 3 grain growth anneal should be about 1025 to 1050°C to provide a sufficient (15%) reserve in the $P_{1.0}$ core loss at the practical maximum line speed of 80 m/min. When this line operating condition is coupled with the resultant grain sizes, an estimate for the desired grain size can be made which in this case is about 60 to 70 μm .

HDPS Dynamo Line Decarburization Simulation—Experimental Procedures.

A similar procedure to that used for the grain growth simulation was adopted. Full-width sheet samples of the commercially produced M400-50A grade were secured following rolling. The cold bands were shipped to the Monroeville Research and Technology Center and were sheared into the HDPS panels. A decarburization soak temperature of 850°C was used with an atmosphere

of 13% H₂ HNX gas with a dew point of about 19°C, yielding a hydrogen to water ratio of about 0.17 to 0.18. After the decarburization anneal was complete, the sample was cooled to room temperature and Soken coupons were prepared. After testing for magnetic properties, the samples were aged for 24 hours at 225°C and retested for calculation of the aging index. Finally, chemical analysis was performed to determine the residual carbon.

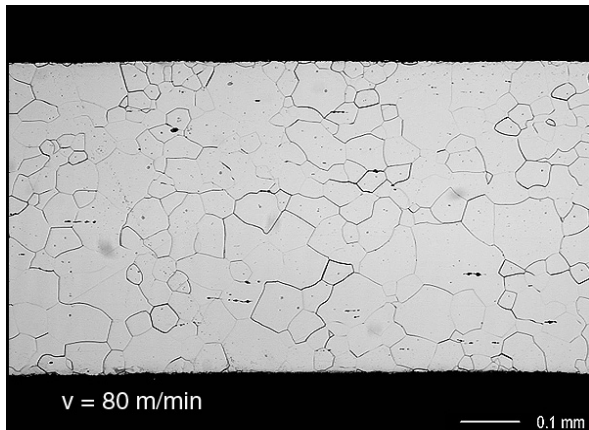


Figure 12a. Longitudinal micrograph at 100X from the center of a Soken test coupon annealed at 1000°C according to a line speed of 80 m/min (15 seconds).

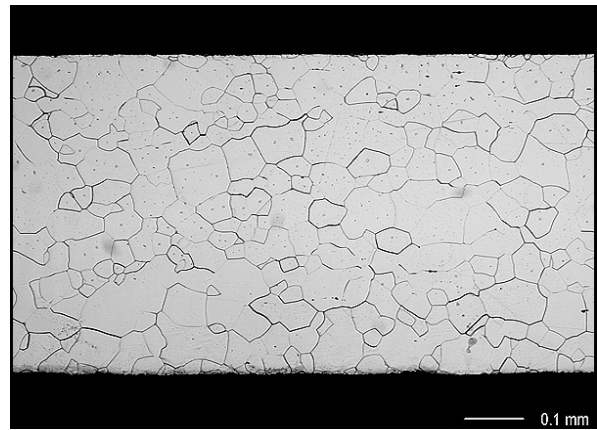


Figure 12b. Longitudinal micrograph at 100X from the corner of a Soken test coupon annealed at 1000°C according to a line speed of 80 m/min (15 seconds).

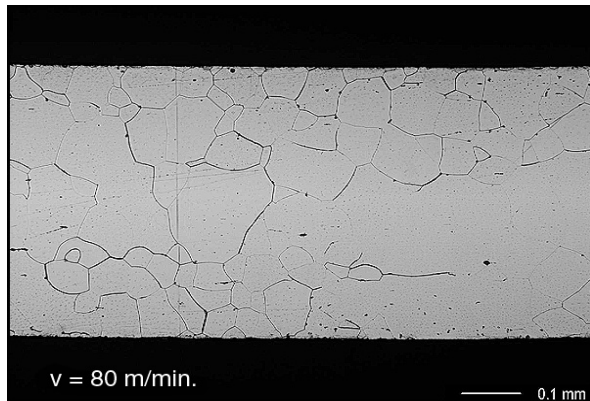


Figure 12d. Longitudinal microstructure at 100X from the center of Soken test coupon annealed at 1045°C according to a line speed of 80 m/min.

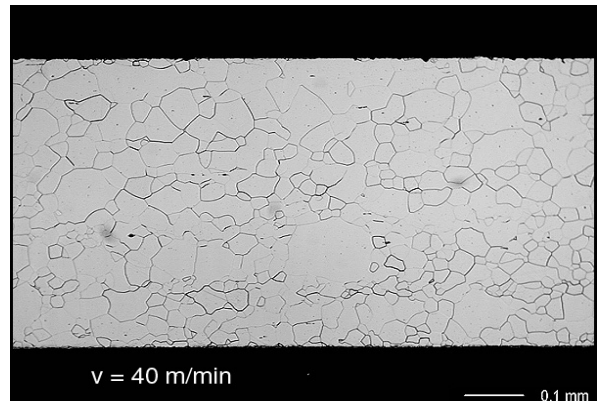


Figure 12c. Longitudinal microstructure at 100X from the center of Soken test coupon annealed at 900°C according to a line speed of 40 m/min.

HDPS Dynamo Line Decarburization Simulation—Results and Discussion.

Figures 13a and 13b show the $P_{1.0}$ and $P_{1.5}$ core losses and J_{2500} and J_{5000} polarizations, respectively, along with the aging index as a function of decarburization soak time. It is clear that as the soak time is increased, the core loss improves and carbon is removed as evidenced by the decline in aging index. Polarization is improved as soak times increase to 75 seconds and then gradually decrease with further increases in the soak time. This is probably the result of an increase in grain size and, for long soak times, the formation of a slight subsurface oxide layer. After a residence time in the decarburization furnace of about 90 seconds, sufficient carbon has been removed to render the material non-aging.

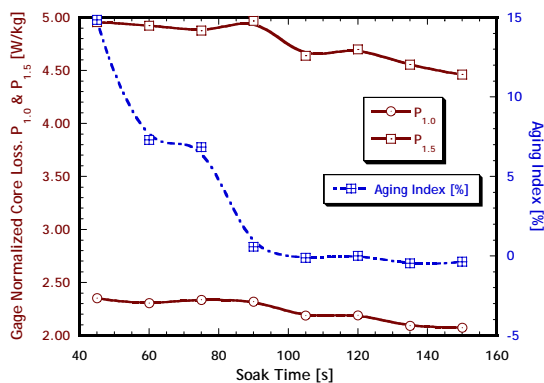


Figure 13a. Core loss and aging index versus soak time for decarburization at 850°C in 13% H₂ HNX gas with a 19°C dew point.

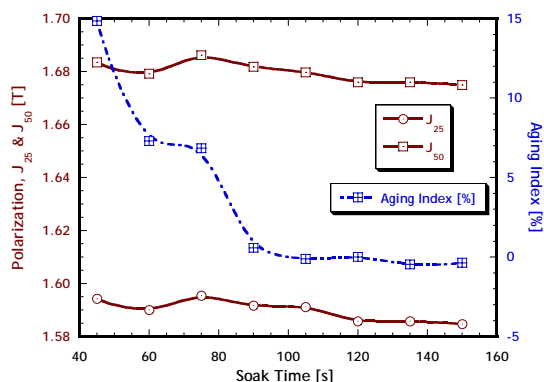


Figure 13b. Polarization and aging index versus soak time for decarburization at 850°C in 13% H₂ HNX gas with a 19°C dew point.

The 105 second soak time results are compared to those from the decarburized starting material used for the grain growth study in Table 7. Very good agreement was obtained between the commercial production and simulation results with $P_{1.0}$ and $P_{1.5}$ core losses not varying by more than 0.05 W/kg and J_{2500} and J_{5000} values being 0.01 higher in the HDPS decarburized material. Figure 14 shows the aging index as a function of the residual carbon levels. It is clear from the figure that carbon levels less than about 60 to 65 ppm yield non-aging material for this grade. This result was surprising as it was expected that residual carbon levels below at least 50 ppm would be required to suppress magnetic aging. The slightly higher than expected carbon threshold for magnetic aging may be related to the differences in aging treatment. In the United States, the 150°C for 100 hour aging treatment is more commonly used rather than the 225°C for 24 hour treatment.

Table 7. Comparison of Post Decarburization Magnetic Properties.

	DN2 Results	HDPS Results
$P_{1.0}$ [W/kg]	2.133	2.188
$P_{1.5}$ [W/kg]	4.658	4.635
J_{2500} [T]	1.581	1.591
J_{5000} [T]	1.669	1.679
Aging Index [%]	0.00	-0.14

Properties measured at 50 Hz.

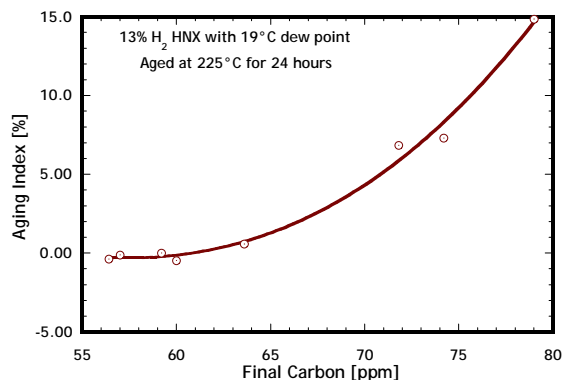


Figure 14. Aging index as a function of the post-decarburization residual carbon level.

The experimental decarburization results were compared to those from a model for the relative change in average carbon for a slab of semi-thickness,⁽²⁾ provide the governing equation as, where C_i is the initial carbon concentration, C_s

$$\bar{C} = [(C_i - C_s) + C_s] \cdot \frac{8}{\pi^2} \cdot \sum_{n=0}^{\infty} \frac{1}{(2n+1)^2} \exp\left[\frac{-(2n+1)^2 \pi^2}{4} \cdot \frac{Dt}{L^2}\right]$$

is the carbon concentration at the surface, D is the diffusivity of carbon in ferrite, t is the soak time, and L is the half thickness of the sheet (0.25 mm in this case). Two diffusivity expressions were used, one by⁽³⁾ for carbon diffusion in α -iron and one by⁽⁴⁾ for carbon diffusion in ferritic electrical steels. The expressions are:

$$D_{Smith} = 0.062 \cdot \exp\left(\frac{-21672}{RT}\right)$$

and

$$D_{Oldani} = 0.020 \cdot \exp\left(\frac{-20100}{RT}\right),$$

where T is temperature in Kelvin (1123 K in this case) and R is the universal gas constant. The comparison of results is shown in Figure 15. The models predict a lower carbon content than the measured results. At 105 seconds the disparity is about 30 ppm carbon. Although there is not good agreement between the actual and theoretical carbon values, this did not seem to affect the agreement in magnetic properties, as presented in Table 7. This is perhaps the more important result as decisions concerning production line operating parameter setups will be made on the basis of magnetic properties, rather than residual carbon levels.

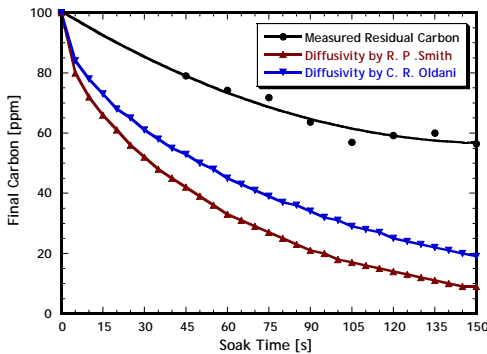


Figure 15. Comparison of actual to model decarburization times.

The 850°C decarburization anneal was then linked with the 1000°C grain growth anneal. The entire Dynamo Line 3 annealing process was simulated using the commercial cold-roll, full-hard M400-50A sheets. A simulated line speed of 50 m/min, giving respective decarburization and grain growth soak times of 100 and 23 seconds, was used. The results from this process simulation are compared against those from the grain growth simulation in Figures 16a and 16b for core loss and polarization, respectively. The $P_{1.0}$ and $P_{1.5}$ core losses match almost exactly those obtained in material decarburized on a production line and then annealed on the HDPS. The polarization results from the HDPS decarburized material are about 0.01 T lower than those obtained with the commercially decarburized M400-50A. The HDPS simulation also adequately decarburized the samples as the aging index varied from about -2.5 to 1.5%.

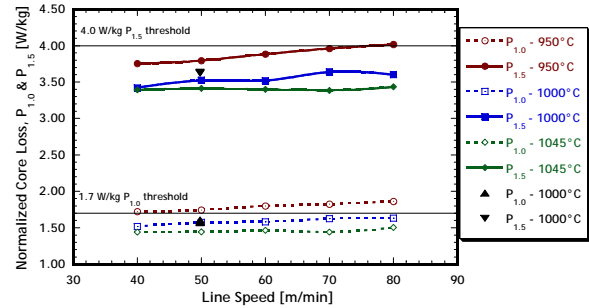


Figure 16a. Core loss results from the full DN3 processing simulation performed on the HDPS. The black triangles are the new results.

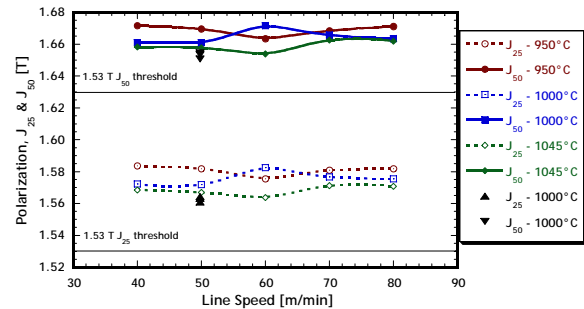


Figure 16b. Polarization results from the full DN3 processing simulation performed on the HDPS. The black triangles are the new results.

Finally, an experiment was conducted in which the HDPS was used to process cold-rolled, full-hard

commercial M400-50A material using the operating parameters of Dynamo Line 3 (DN3). Table 8 compares these key operating parameters to those used on the HDPS. The core loss and polarization results are also shown in Table 8. Again, very good agreement is seen between the production and simulated process magnetic property results. The HDPS $P_{1.5}$ core losses tend to be about 0.2 to 0.3 W/kg lower than those

generated on Dynamo Line 3. The J_{5000} magnetic polarization results are also close, with a difference of about 0.01 to 0.015 T. Considering the operational differences between a production Dynamo Line and the HDPS and the magnetic property measurement correlations, this agreement is considered to be quite good. The HDPS is now being used to aid development of electrical steel grades as well as zinc-coated steels.

Table 8. Comparison of DN3 and HDPS Processing Conditions and Resultant Magnetic Properties.

Conditions/Properties	DN3	HDPS	HDPS
Line Speed	45	45	45
Decarburization Temperature [°C]	830-850	825	850
Decarburization H ₂ O/H ₂ ratio	0.15	0.15	0.15
Grain Growth Temperature [°C]	1060	1000	1000
$P_{1.0}$ [W/kg]	1.63	1.48	1.51
$P_{1.5}$ [W/kg]	3.79	3.56	3.51
J_{2500} [T]	1.575	1.591	1.586
J_{5000} [T]	1.667	1.684	1.677
Aging Index [%]	0.21	1.38	2.81

Properties measured at 50 Hz.

Conclusions.

A simulation of the decarburization and grain growth anneals from a commercial electrical steel processing line has been accomplished using a hot dip process simulator. Because of limited sample size, a small single sheet tester, the Soken DAC-BHW5, was used to evaluate the magnetic properties. A correlation was developed between Soken and Epstein magnetic properties using commercially-produced fully-processed electrical steels. Correlations between Soken and Epstein core losses were found to be linear and nearly the same for longitudinal and transverse directions. The effect of grade on the core loss correlation was slight and was ignored, however gage effects could not be ignored. Therefore, separate correlations were built for gages of 0.50 and 0.65 mm. As was found for core loss, the correlations for magnetic flux density included gage and test orientation but not grade. The arithmetic average of Epstein correlated longitudinal and transverse properties was used to provide composite (longitudinal and transverse) Epstein results. The deviation between Epstein equivalent and Epstein measured 1 and 1.5 Tesla core losses and the magnetic flux densities

B_{800} , B_{2500} , and B_{5000} were within 3% and 1% respectively.

The HDPS provided an accurate simulation of the grain growth anneal over temperatures ranging from 900 to 1045°C at simulated line speeds ranging from 40 to 80 m/min. The initial value of the $P_{1.5}$ core loss of 4.66 W/kg (the average from the head, middle and tail coil locations after decarburization) was reduced to 3.38 to 4.29 W/kg depending upon the annealing condition. The annealing time-temperature-property results showed that increasing the temperature of the grain growth anneal and prolonging the soaking time lead to the expected decrease in core losses. For this M400-50A grade, the 1.70 W/kg maximum $P_{1.0}$ core loss is more difficult to meet than the 4.00 W/kg $P_{1.5}$ core loss. The effect of soak time on core loss is not especially strong, as increasing the line speed from 40 to 80 m/min only increases core losses by about 0.3 W/kg. For the J_{2500} and J_{5000} polarizations, all of the grain growth annealing conditions produced magnetic flux density values substantially above the minimum specified levels of 1.53 and 1.63 T, respectively. Optical

microstructures from the center and one corner of the 3-in. by 3-in. Soken test coupons were compared and it was concluded that the grain size difference was slight and not significant. Therefore, the magnetic property variability within the coupon due to grain size differences is not believed to be significant. The grain size following the decarburization anneal, estimated to be about 20 μm , increased to about 23 μm to 70 μm following the various grain growth anneal simulations. In reviewing all of the magnetic property information, the estimated strip temperature for the Dynamo Line 3 grain growth anneal should be about 1025 to 1050°C to provide a sufficient reserve in the P_{1.0} core loss at the practical maximum line speed of 80 m/min. The corresponding final grain size for this line condition is about 60 to 70 μm .

A similar procedure to that used for the grain growth simulation was adopted for the decarburization simulation. A decarburization soak temperature of 850°C was used with an atmosphere of 13% H₂ HNX gas with a dew point of about 19°C yielding a hydrogen to water ratio of about 0.17 to 0.18. After a residence time in the decarburization anneal of about 90 seconds, sufficient carbon has been removed to render the material non-aging. As the soak time is increased, the core loss continually improves. Magnetic polarization is improved as soak times increase to 75 seconds and then gradually decrease with further increases in the soak time. This is probably the result of an increase in grain size and, for long soak times, the formation of slight subsurface oxide layer. The experimental carbon removal results did not agree with those predicted from a diffusion model of a semi-infinite slab. They were about 30 ppm higher than predicted for the 105 second soak. However, very good agreement was obtained between the commercial production and simulation magnetic properties following decarburization annealing with P_{1.0} and P_{1.5} core losses not varying by more than 0.05 W/kg and J₂₅₀₀ and J₅₀₀₀ values being 0.01 higher in the HDPS decarburized material. For this grade of M400-50A material, the carbon level must be lower than 60 to 65 ppm for the material to be non-aging. The decarburization and grain growth simulations were

linked so that the entire electrical steel annealing process was modeled. Magnetic properties from material given the entire electrical steel annealing simulation were compared to those obtained on commercially produced material. Very good agreement was obtained with the HDPS P_{1.5} core losses tending to be about 0.3 W/kg lower. The J₅₀₀₀ magnetic polarization results were very close, having a difference of only 0.01 to 0.015 T. The HDPS is now being used to aid development of electrical steel grades.

The material in this paper is intended for general information only. Any use of this material in relation to any specific application should be based on independent examination and verification of its unrestricted availability for such use, and a determination of suitability for the application by professionally qualified personnel. No license under any United States Steel Corporation patents or other proprietary interest is implied by the publication of this paper. Those making use of or relying upon the material assume all risks and liability arising from such use or reliance.

References.

- (1) Larsen, A. M. R. Blotzer, R. J. Lauer, B. A. and Anderson, J. P. 2005. Magnetic Testing Methods for Motor Lamination Steels. *Proceedings of the 12th Conference on Properties and Applications of Magnetic Materials, May 18th – 20th, 2005.* Illinois Institute of Technology, Chicago.
- (2) Oldani, C. R. 1996. Decarburization and Grain Growth Kinetics During the Annealing of Electrical Steels. *Scripta Materialia*. 35 (11) : 1253-1257.
- (3) Poirier, D. R. and Geiger, G. H. *Transport Phenomena in Materials Processing*, TMS, Warrendale, Pennsylvania : 447.
- (4) Smith, R. P. 1962. The Diffusivity of Carbon in Alpha-Iron. *Transactions of the AIME*, 224 (Feb) : 105-111.

